AJNR

Brain Arteriovenous Malformations: Assessment with Dynamic MR Digital Subtraction Angiography

Paul D. Griffiths, Nigel Hoggard, Daniel J. Warren, Iain D. Wilkinson, Bob Anderson and Charles A. Romanowski

AJNR Am J Neuroradiol 2000, 21 (10) 1892-1899
http://www.ajnr.org/content/21/10/1892

AJNR Am J Neuroradiol 21:1892–1899, November/December 2000

Brain Arteriovenous Malformations: Assessment with Dynamic MR Digital Subtraction Angiography

Paul D. Griffiths, Nigel Hoggard, Daniel J. Warren, Iain D. Wilkinson, Bob Anderson, and Charles A. Romanowski

BACKGROUND AND PURPOSE: **Conventional catheter angiography (CCA) is the current reference standard for the diagnosis, assessment, and management of pial brain arteriovenous malformations (AVMs). The purpose of this study was to develop an MR angiographic technique that produces dynamic images comparable to those provided by CCA and to apply the technique to the investigation of pial brain AVMs.**

METHODS: **Twenty patients with brain AVMs referred for stereotactic radiosurgery were recruited. All patients had CCA performed on a 1.5-T superconducting system. Sixty images were obtained at a rate of one image per second. Slices were orientated to produce Towne, lateral, and anteroposterior projections. A set of mask images was taken and then a series during the passage of a bolus of contrast material. MR examinations were assessed independently by neuroradiologists blinded to the conventional catheter angiographic findings.**

RESULTS: **The nidus of the AVMs was depicted in 19 of the 20 patients, and correlation with CCA was excellent for measurements of maximum diameter. Venous drainage was correctly assessed in 18 of 19 cases.**

CONCLUSION: **MR digital subtraction angiography shows promise as a noninvasive, dynamic angiographic tool for planning stereotactic radiosurgery of AVMs already delineated by catheter angiography. At present, it suffers from temporal and spatial resolution, which impede the assessment of some brain AVMs.**

Arteriovenous malformations (AVMs) are nonneoplastic vascular abnormalities that are considered to be congenital lesions by most authorities. Cerebral pial AVMs are found in approximately 0.1% of the North American population (1). Although they may be incidental findings at neuroimaging, they are an important cause of nontraumatic intracranial hemorrhage in both adults and children. Nonhemorrhagic presentations include seizures, focal neurologic deficits, and headaches (2). When AVMs are detected, treatment is usually offered because of the high risk of future hemorrhage, which has been reported as being between 2% and 4% per year if left untreated (3–11). Conventional neurosurgery, endovascular treatment, stereotactic radiosurgery, or combinations of the three are used in most circumstances.

Our center is a national institute for radiosurgery and treats 300 to 350 brain AVMs per year. Most patients are referred to our center with the diagnosis of AVM already made on the basis of conventional catheter angiography (CCA). However, we repeat CCA to plan the stereotactic procedure and, subsequently, to evaluate the response to radiosurgery. Ideally, this should be done by noninvasive methods, such as MR angiography, because of the small but finite risk of a permanent neurologic deficit developing after CCA, which occurs with a frequency of 0.1% to 1.0% (12–17).

Standard MR imaging and MR angiography can confirm the presence of an AVM. But, currently, MR angiography does not provide sufficiently accurate nidal definition on which to make clinical decisions or plan treatment. The main advantage CCA has over time-of-flight (TOF) MR angiography, besides superior spatial resolution, is the provision of dynamic information, which helps to distinguish the nidus from draining veins (18).

In this article, we describe our early experience with an experimental dynamic MR angiographic method using a contrast agent and a digital mask for cerebral AVM assessment. The technique has been described as MR digital subtraction angiography (MR-DSA) (19, 20).

Methods

During a 4-month period, 20 consecutive patients with angiographically confirmed brain AVMs, referred to our institu-

Received March 6, 2000; accepted after revision May 9.

From the Academic Department of Radiology, University of Sheffield, MRI Department, Royal Hallamshire Hospital, Glossop Rd, Sheffield, South Yorkshire, S10 2JF, U.K. Address reprint requests to Professor P. D. Griffiths.

tion for stereotactic radiosurgery, were recruited into this study. The patient population consisted of 11 male and nine female patients ranging in age from 15 to 62 years (median age, 36 years). Eleven patients presented initially with hemorrhage, six with seizures, two with headache, and one with a progressive right-sided weakness. Nine of the patients had undergone previous embolization treatment, and one had also undergone a craniotomy and open surgery. A further two had had previous partially successful stereotactic radiosurgery.

All MR imaging was performed on a 1.5-T superconducting system with 27-mT/m maximum gradient strength used in conjunction with a head coil. All patients were referred for MR imaging, in keeping with accepted clinical practice at our institution, and informed consent was obtained in all cases. Axial dual-echo images were obtained with a fast spin-echo sequence at 2900/87.5,12.5 (TR/TE), a 256 × 192 matrix, a 90° flip angle, a 23-cm field of view (FOV), and a 5-mm slice thickness with a 2-mm interslice gap. Sampling bandwidth was 20.83 kHz and the phase sampling ratio was 0.820.

MR-DSA methodology was modified from Aoki et al (19). Sixty images were obtained using an RF-spoiled 2D Fourier-transformation steady-state technique, which permits one image per second. Imaging parameters for the gradient-echo sequence were 7/2 (TR/TE), a 40° flip angle, a 23-cm FOV, a 256 × 150 matrix, and a slice thickness of 6 to 10 cm. The phase sample ratio was 1.0 and the bandwidth was 50.0 kHz. Slices were orientated to give projections equivalent to those produced by CCA. In any given imaging domain (axial, lateral, reverse Towne), one run was conducted as a mask and a second run was obtained during the passage of a bolus of 6 to 10 mL (concentration, 0.5 M) of gadopentetate dimeglumine followed by a 10-mL saline flush. A separate contrast bolus was used for each anatomic projection. This was administered at a rate of 3 mL/s via a power injector (Medrad Spectris, Medrad, Netherlands) through an 18-gauge intravenous cannula inserted into the antecubital fossa vein (21). The quantity of contrast material varied according to nidus size, as determined from the standard fast spin-echo images, to optimize nidus visualization: 6 mL of full-strength gadopentetate dimeglumine was used for small (<3 cm) AVMs and 10 mL for medium-sized (3–6 cm) AVMs. After imaging, the mask run for a particular imaging plane was subtracted from the contrast run using proprietary software, and then viewed using video reversed cine. A maximum of 20 mL of gadopentetate dimeglumine was administered to any one patient.

CCA was conducted pretherapeutically under stereotactic conditions. A Leksell model G stereotactic coordinate frame (Elekta Instruments, Atlanta, GA) was secured to the patient's head using a local anesthetic at the four sites of pin insertion. Limited selective transfemoral cerebral angiography was performed, and standard film-screen techniques and intraarterial digital subtraction were used to obtain anteroposterior, lateral, and oblique views. Images were printed with a 512 × 512 matrix, a 1- to 7-cm FOV in the anteroposterior plane, and a 25-cm FOV in the lateral plane. Dose planning was performed with Gammaplan software (Elekta Instruments), which enabled radiographic magnification factors to be accounted for and used as a basis for subsequent measurements of nidal size.

There are several ways of classifying brain AVMs, but the most widely accepted was put forward by Spetzler and Martin (22), who scored AVMs with respect to nidus size, type of venous drainage, and anatomic eloquence. In our study, the location of the AVM was determined from cross-sectional imaging, as is current working practice, and assessment of MR-DSA images was based on the standard Spetzler-Martin criteria. Note was also made of the presence or absence of any associated vascular anomalies.

The association of intracranial aneurysms with AVMs has been well documented in the literature (23, 24). A widely accepted system for categorizing the AVM-aneurysm relationship, however, has yet to be established. Our classification follows that proposed by Redekop et al (23), who categorized aneurysms as intranidal, flow-related, or unrelated to the AVM. In keeping with this classification, intranidal aneurysms are those that fill early, before substantial venous filling occurs, and are localized within the boundary of the nidus. Venous pouches, venous dilatations, and simple angiomatous changes were excluded.

Two trained observers, both blinded to the results of either study, retrospectively reviewed both the CCA and MR-DSA images independently. Cases were reviewed randomly, and conflicting interpretations were resolved by consensus.

AVM size was described in three dimensions: craniocaudal and anteroposterior measurements were determined on a lateral view and mediolateral measurements on an anteroposterior or Towne view. The maximum linear dimension of the AVM nidus was compared with CCA findings, and the standard correlation coefficient was obtained for the two techniques. Deep venous drainage was graded as either present or absent.

Results

Twenty-one AVMs were found in the 20 patients. One patient had bilateral, mirror-image parietal AVMs, only one of which was considered for stereotactic radiosurgery; the second AVM was not included in further analysis (Fig 1). The anatomic locations of the 20 AVMs are listed in Table 1. Nineteen of the 20 AVMs were considered to be eloquent. An AVM of the corpus callosum is shown in Figure 2. Table 2 summarizes the findings by both observers. MR-DSA depicted 19 of the 20 AVMs, giving a sensitivity of 95% for nidus detection. Both observers missed a 10-mm AVM in the right temporal lobe. Although the abnormality was apparent at CCA, the findings were considered to be subtle. The AVM was delineated on MR images only by the presence of a slightly enlarged draining vein.

Determination of Nidus Size

Figure 3 is a scatter plot comparing nidus size as represented by MR-DSA and CCA. The results show reasonable agreement between the three orthogonal plane measurements and excellent correlation between the maximum linear dimension that was used for the Spetzler grading (Pearson correlation coefficient, $r = .953$, $P = .01$). The MR-DSA axial images (see Fig 4) were not used in this analysis, as there were no equivalent CCA projections for comparison. In the 19 AVMs shown by both methods, there was complete agreement between CCA and MR-DSA for classification of nidus size: 13 were identified as small (<3 cm) and six as medium sized (3–6 cm).

Venous Drainage

CCA showed 12 AVMs to have superficial venous drainage only and eight to have both deep and superficial drainage. As described previously, MR-DSA failed to show one AVM. Of the other 19, MR-DSA and CCA findings agreed in 18 of 19 cases. In one case, MR-DSA incorrectly showed

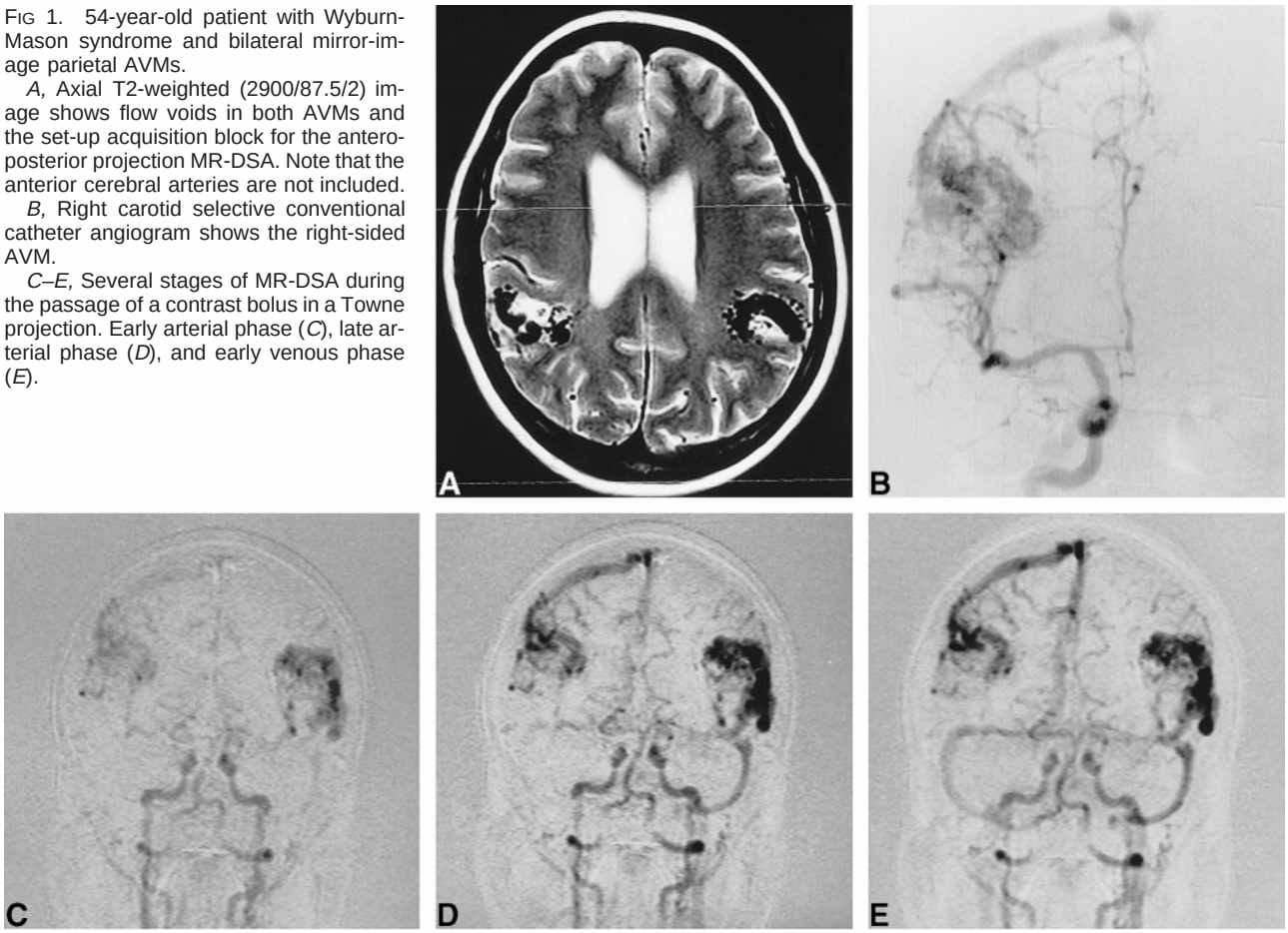

FIG 1. 54-year-old patient with Wyburn-Mason syndrome and bilateral mirror-image parietal AVMs.

A, Axial T2-weighted (2900/87.5/2) image shows flow voids in both AVMs and the set-up acquisition block for the anteroposterior projection MR-DSA. Note that the anterior cerebral arteries are not included.

B, Right carotid selective conventional catheter angiogram shows the right-sided AVM.

C–E, Several stages of MR-DSA during the passage of a contrast bolus in a Towne projection. Early arterial phase (*C*), late arterial phase (*D*), and early venous phase (*E*).

TABLE 1: Anatomic locations of 20 arteriovenous malformations

Location	No. of Cases (%)
Supratentorial	18 (90)
Lobar	13 (65)
Frontal	1
Parietal	3
Temporal	3
Occipital	2
Multilobar	4
Basal ganglia	4 (20)
Corpus callosum	1 (5)
Infratentorial	2 (10)
Cerebellum	2 (10)

deep venous drainage that was not confirmed by CCA.

Spetzler-Martin Grade

From the previous results, it is possible to compare MR-DSA and CCA in terms of the Spetzler-Martin classification system. Eighteen of the 20 AVMs were correctly classified by MR-DSA findings: eight were grade II, seven were grade III, and three were grade IV. The AVM not seen at MR-DSA was a grade II lesion, and one grade II AVM was incorrectly classified as grade III.

Associated Vascular Anomalies

Flow-related aneurysms were seen in two (10%) of the 20 cases. In one case, a right pericallosal artery aneurysm was seen by both observers on MR-DSA images and was shown with a second anterior communicating artery aneurysm, agreed upon after review, on CCA images (Fig 5). In the second case, a left cerebellar AVM was shown to have multiple feeding arteries on both CCA and MR-DSA images. Neither observer reported a false-positive finding on MR-DSA images. CCA showed one AVM to have a small intranidal aneurysm that was not seen by either observer on the MR-DSA images. No unrelated aneurysms were depicted by either technique.

Discussion

The risk of complications from catheter angiography in young or middle-aged patients with brain AVMs is low. Nonetheless, the development of noninvasive angiographic techniques remains a justifiable goal in terms of cost, radiation protection, and patient comfort. Owing to the low risk of cerebral

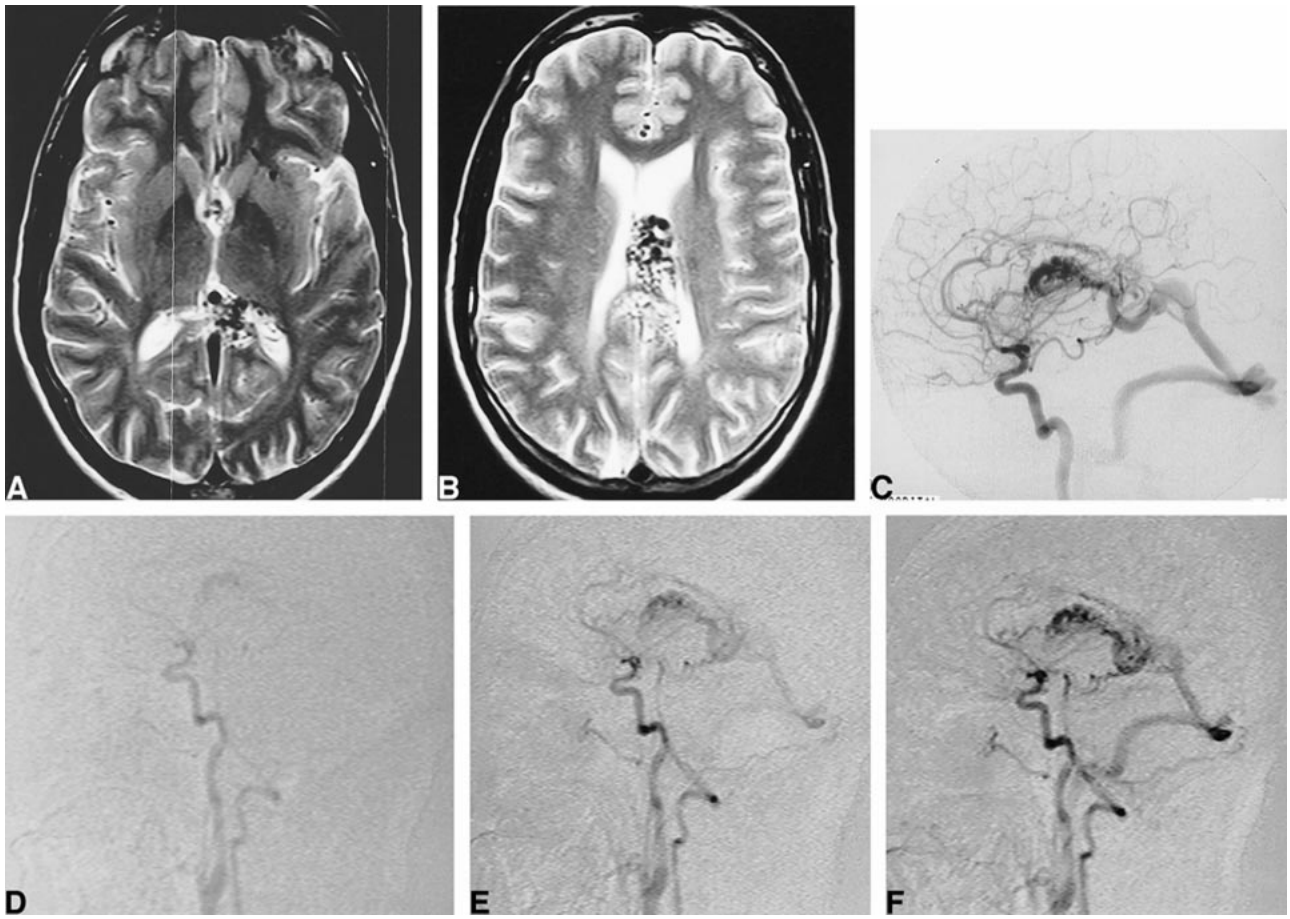

FIG 2. 36-year-old man with a corpus callosum AVM that extends into the left lateral ventricle.
A, Axial T2-weighted (2900/87.5/2) image though the level of the nidus with set-up acquisition block for lateral projection MR-DSA.
B, T2-weighted image shows the nidus extending into the left lateral ventricle.
C, Left carotid selective conventional catheter angiogram shows the AVM.
D–F, Several stages of MR-DSA during passage of a contrast bolus in a lateral projection. Early arterial phase (*D*), late arterial phase (*E*), and early venous phase (*F*).

angiography in patients with AVMs, the diagnostic accuracy of noninvasive imaging techniques, such as MR angiography and CT angiography, must be comparable to that of CCA if they are to be used as a substitute for CCA (25).

During the 1980s, MR angiography emerged as an important radiologic tool and, at the forefront, was TOF MR angiography (26). Three-dimensional TOF MR angiography permits 3D delineation of the vascular architecture and, as such, has proved to be of great value in many neuroradiologic scenarios. MR angiography, in conjunction with CCA, is used in planning stereotactic radiosurgery and radiation dose at many neurosurgical centers (18, 27). CCA images provide only a 2D projection of the 3D nidus, which introduces many problems, including making it difficult to define the medial contour. This can occasionally compromise nidal assessment, which may result in a suboptimal radiation dose. Developers of new imaging techniques must balance their ultimate goal of gaining optimal diagnostic information against the resultant effects on treatment (28). Thus, 3D-TOF MR angiography is an adjunct to CCA, but not a replacement. It has been shown that when this technique is used to image brain AVMs, it cannot consistently depict small vessels and regions of slow blood flow (26). Slow flow, whether in small arteries or draining veins, results in saturation from repeated RF pulses and subsequent loss of clarity of vessel delineation (29, 30). This is complicated by the anatomy of the nidus, in which multidirectional flow causes further signal saturation, making arterial and venous differentiation difficult and highly subjective (18, 31). The use of the T1 shortening property of gadopentetate dimeglumine helps to overcome the saturation effects of slow flow (26). Three-dimensional TOF MR angiography also suffers from a lack of dynamic information; the presence of an early draining vein is sufficient to diagnose AVMs on CCA images and this is often not possible on TOF studies. Hence, there are significant problems in assessing AVMs by TOF MR angiography.

Radiosurgery may take from 2 to 3 years to obliterate brain AVMs completely; however, good results are common, with 80% of patients showing complete angiographic obliteration after this latency period (11, 32–37). Complete obliteration has

TABLE 2: Summary of findings in 20 patients with arteriovenous malformations

	MR Imaging (Observer 1)	Digital Subtraction Angiography (Observer 2)	MR Imaging/ Digital Subtraction Angiography Consensus	Conventional Catheter Angiography	Intertechnique Agreement (%)
Demonstration of nidus	19/20	19/20	19/20	20/20	95
Nidus size					
<3 cm	13/20	13/20	13/20	14/20	93
3–6 cm	6/20	6/20	6/20	6/20	100
Venous drainage					
Superficial only	10/20	10/20	10/20	12/20	
Deep only	5/20	4/20	5/20	5/20	90
Superficial and deep	4/20	5/20	4/20	3/20	
Spetzler grade					
II	8/20	8/20	8/20	10/20	
III	8/20	8/20	8/20	7/20	90
IV	3/20	3/20	3/20	3/20	
Aneurysms					
Flow-related	2/2	2/2*	2/2	2/2	100
Intranidal	0/1	0/1	0/1	1/1	0

* Both patients had multiple aneurysms, one aneurysm in one of the patients was not seen initially by observer 2 but was seen and agreed upon at consensus.

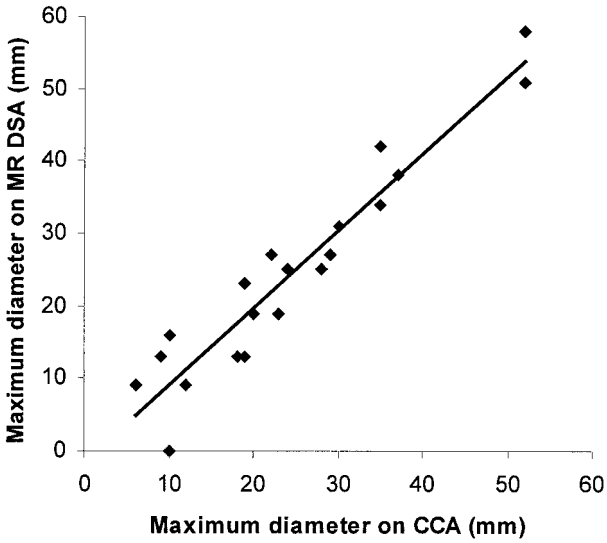

FIG 3. Scatter plot of maximum measured diameter of AVM nidus on MR-DSA against that measured on CCA with the line of best fit shown; calculated Pearson correlation coefficient, $r = .953$, $P = .01$.

been defined by Steinberg et al (38) as ''the absence of any angiographically visible arteriovenous shunt.'' Within the stated latency period there remains a potential risk for hemorrhage (7, 11, 35, 39, 40), and the recognition of complete obliteration is central for further patient management. There are no published data on optimal follow-up procedures after radiosurgery (32), but most institutions offer follow-up CCA 2 years after treatment. This will mean a minimum of three angiographic assessments, one for diagnosis, one for prestereotactic planning, and one for follow-up. MR-DSA has potential benefit for noninvasive evaluation of AVMs in diagnosis, radiosurgical dose planning, and posttreatment assessment.

Recent reports have shown that MR-DSA has proved to be capable in providing dynamic angiographic images with a short acquisition time. Wang et al (20) studied the somatic vasculature of 28 patients with dynamic angiographic MR-DSA and contrast enhancement. Hennig et al (41) used a similar technique in 24 patients, and reached a comparable conclusion. Aoki et al (19) showed clear arterial and venous phase separation in 35 cases of cerebrovascular disease, including three brain AVMs.

The use of MR-DSA to study brain AVMs has proved encouraging. A sensitivity of 95% for nidus detection is comparable or superior to that of 3D-TOF MR angiography (42). The limitations at present are the lack of in-plane anatomic resolution and a lengthy acquisition time of one image per second. Because the intracranial circulation has a short time interval between arterial and venous phases, small early draining veins and simple small arteriovenous shunts may be missed. Moreover, the opportunity to acquire high-resolution images is limited (26).

MR-DSA showed 100% correlation with CCA with respect to Spetzler-Martin size classification in 19 of the 20 AVMs visualized. Dynamic imaging is required for accurate nidal measurement in order to separate arterial and venous structures. However, nidal measurement is highly subjective, and as such, further analysis beyond that of Spetzler-Martin grouping is of limited value. A degree of measurement variability is to be expected, not only because of the subjectivity of the measurement but

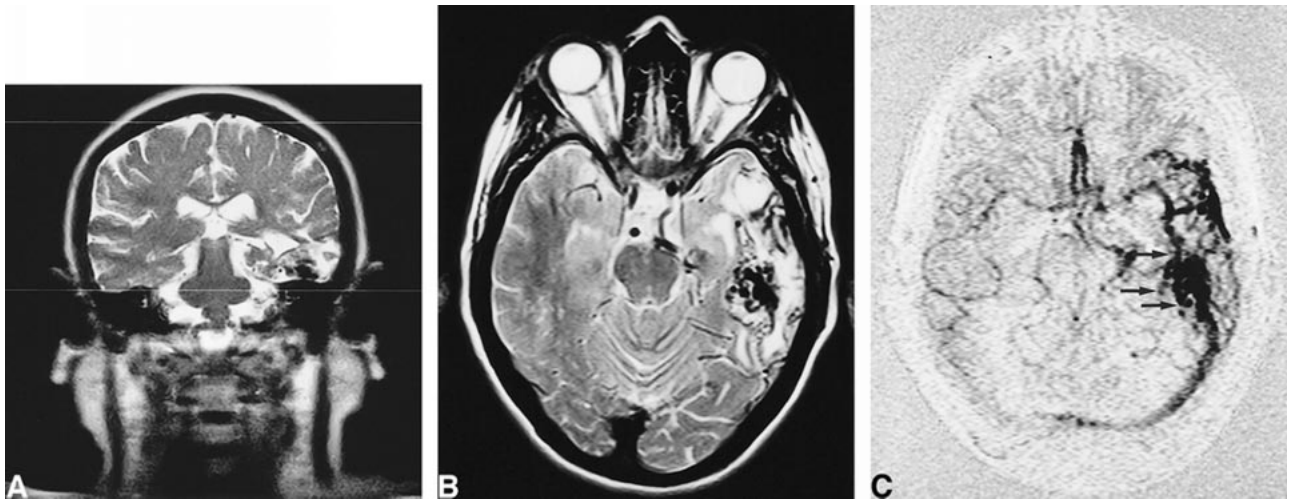

FIG 4. 31-year-old woman with a left temporal lobe AVM.

A, Coronal T2-weighted (2900/75/1) single-shot echo-planar image shows the set-up acquisition block for the axial projection MR-DSA.

B, T2-weighted 2900/87.5/2 axial section through the level of the nidus.

C, Early arterial phase axial projection MR-DSA shows the contour of medial border (*arrows*). This contour cannot be depicted with CCA.

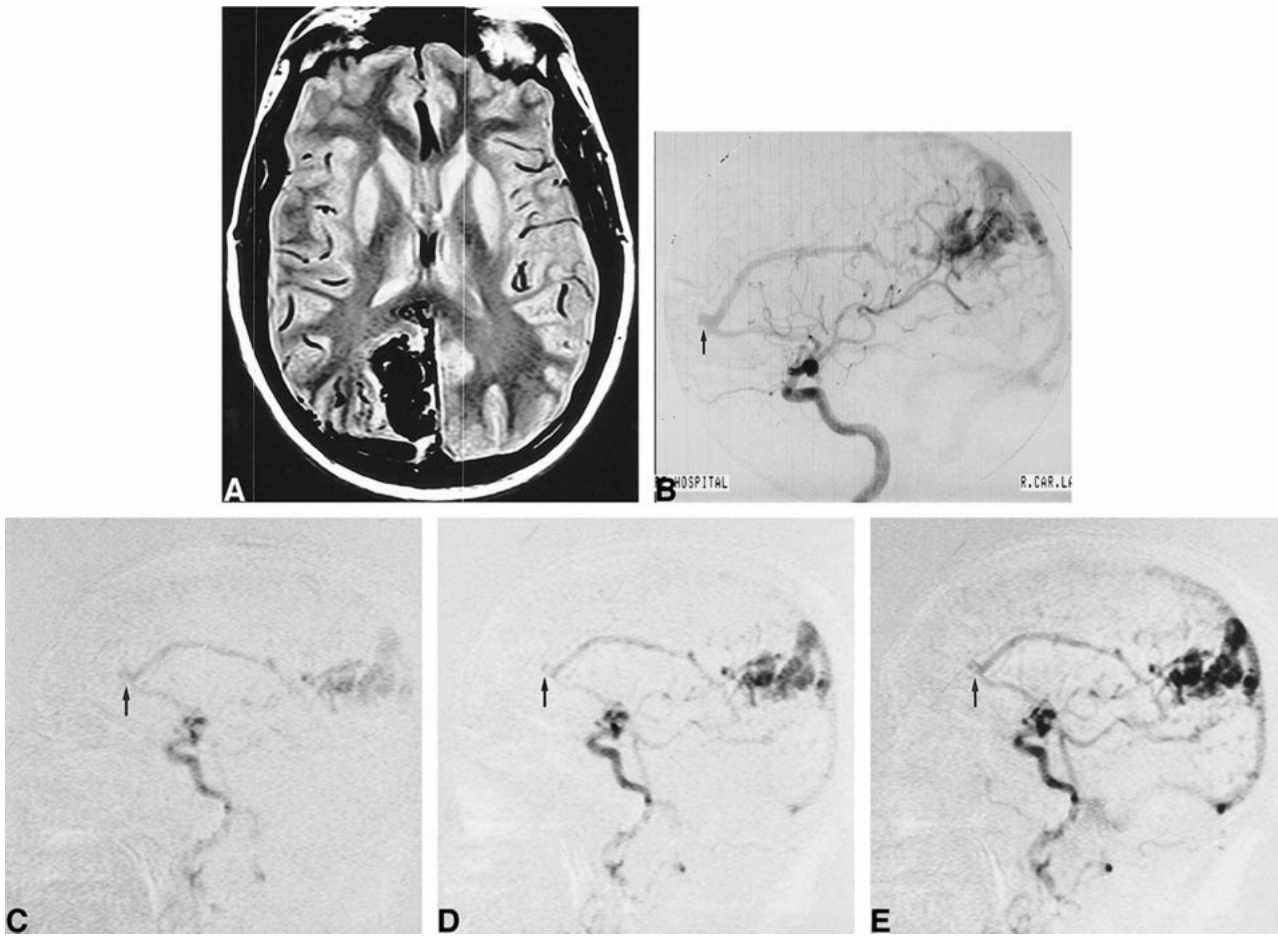

FIG 5. 62-year-old man with an occipitoparietal AVM.

A, Axial T2-weighted (2900/87.5/2) image shows the set-up acquisition block for the lateral projection MR-DSA at the level of the nidus.

B, Lateral projection from a selective right internal carotid conventional catheter angiogram shows a flow-related aneurysm on the pericallosal artery (*arrow*).

C–E, This projection not only shows the nidus in the early arterial phase but also the flow-related aneurysm (*arrow, C*). In addition, there is an anterior communicating artery aneurysm, not well shown on this projection, which was noted by consensus at review. Late arterial phase (*D*), early venous phase (*E*).

also because of the MR-DSA in-plane resolution of 256 × 150 (used for speed optimization) against 512 × 512 resolution of CCA. We found dynamic MR-DSA of value in identifying venous drainage, allowing 90% of AVMs to be correctly graded by the Spetzler classification.

The prevalence of flow-related aneurysms shown in the present study is in keeping with that found in larger series (23, 24). The impact of partial or complete AVM obliteration on the natural history of such aneurysms remains unclear, and thus the need for treatment of an incidentally discovered coexisting aneurysm remains controversial (23). Interpretation of intranidal aneurysms is highly subjective and viewer-dependent (23). Thus, any comparison of imaging methods in this regard is also necessarily highly subjective; for example, in differentiating a late-filling aneurysm from an early-filling venous pouch. Flow aneurysms are more easily defined, and comparisons between MR-DSA and CCA in this regard proved comparable in our study population. However, this success is viewed with a degree of caution. Complete assessment of the intracranial vessels would benefit from superior spatial and temporal resolution, particularly in the assessment of abnormalities associated with AVMs, such as intranidal aneurysms or venous drainage stenoses, which are associated with a higher risk of hemorrhage. Therefore, MR-DSA cannot replace the initial diagnostic study because of those limitations, and we recommend the use of this technique as an adjunct to catheter angiography at the present time.

MR-DSA provides valuable information by producing images in the axial plane (see Fig 4C). Axial images are not obtainable with CCA, and unless standard MR or CT studies are available for planning purposes, the medial contour cannot be planned accurately during stereotactic radiosurgery.

Although gadolinium-based contrast material is safe to use in high volumes, we have not found that this is an advantage with this method. At present, the dose per run is empirically based on the size of the nidus as determined from cross-sectional imaging. The comparatively small volumes of contrast agent that we administered led to better delineation of arterial, nidal, and venous anatomy because of the compactness of the bolus. A further benefit of using a lower volume of gadolinium chelates is the minimization of image degradation after repeated injections for different projections. The combination of low-volume contrast material and a mask method resulted in little discernible loss of image quality on the second or third angiographic run. The use of even smaller volumes of gadolinium chelates with higher concentrations should improve the technique.

Conclusion

The technique described in this article cannot replace CCA at present. CCA combines superb anatomic resolution (approximately 0.5 mm when using a 512 matrix or 0.25 mm when using a 1024 matrix, with a 25-cm FOV) with excellent temporal resolution. Most centers rely on four to six frames per second when assessing AVMs, and many modern angiographic units can produce 24 frames or more per second. The MR-DSA technique described here used a 256 matrix and an acquisition time of one frame per second, which limited its diagnostic utility. Our initial results with MR-DSA are encouraging, but further improvements are required before we can draw firm conclusions regarding its usefulness in planning radiosurgery and in accurately confirming nidal involution.

Acknowledgment

We acknowledge the input of Marconi Medical Systems, which is a research partner.

References

1. Brown RD Jr, Wiebers DO, Torner JC, O'Fallon WM. **Frequency of intracranial hemorrhage as a presenting symptom and subtype analysis: a population based study of intracranial vascular malformations in Olmsted County, Minnesota.** *J Neurosurg* 1996;85:29–32
2. Wilkins RH. **Natural history of intracranial vascular malformations: a review.** *Neurosurgery* 1985;16:421–430
3. Brown RD, Wiebers DO, Forbes G, et al. **The natural history of unruptured intracranial arteriovenous malformations.** *J Neurosurg* 1988;68:352–357
4. Crawford PM, West CR, Chadwick DW, et al. **Arteriovenous malformations of the brain: natural history in unoperated patients.** *J Neurol Neurosurg Psychiatry* 1986;49:1–10
5. Fults D, Kelly DL Jr. **Natural history of arteriovenous malformations of the brain: a clinical study.** *Neurosurgery* 1984;15: 658–662
6. Graf CJ, Perret GE, Torner JC. **Bleeding from cerebral arteriovenous malformations as part of their natural history.** *J Neurosurg* 1983;58:331–337
7. Itoyama Y, Uemura S, Ushio Y, et al. **Natural course of unoperated intracranial arteriovenous malformation: study of 50 cases.** *J Neurosurg* 1989;71:805–809
8. Forster DMC, Steiner L, Hakanson S. **Arteriovenous malformations of the brain: a long-term clinical study.** *J Neurosurg* 1972;37:562–570
9. Auger RG, Wiebers DO. **Management of unruptured intracranial arteriovenous malformations: a decision analysis.** *Neurosurgery* 1992;30:561–569
10. Hartmann A, Mast H, Mohr JP, et al. **Morbidity of intracranial hemorrhage in patients with cerebral arteriovenous malformation.** *Stroke* 1998;29:931–934
11. Pollock BE, Flickinger JC, Lunsford LD, Bissonette DJ, Kondziolka D. **Hemorrhage risk after stereotactic radiosurgery of cerebral arteriovenous malformations.** *Neurosurgery* 1996;38: 652–661
12. Pollock BE, Kondziolka D, Lunsford LD, et al. **Repeat stereotactic radiosurgery of arteriovenous malformations: factors associated with incomplete obliteration.** *Neurosurgery* 1996;38: 318–324
13. Grzyska U, Freitag J, Zeumer H. **Selective cerebral intraarterial DSA: complication rate and control of risk factors.** *Neuroradiology* 1990;32:296–299
14. Heiserman JE, Deam BL, Hodak JA, et al. **Neurologic complications of cerebral angiography.** *AJNR Am J Neuroradiol* 1994; 15:1401–1407
15. Waugh JR, Sacharias N. **Arteriographic complications in the DSA era.** *Radiology* 1992;182:243–246
16. Dion JE, Gates PC, Fox AJ, et al. **Clinical events following neuroangiography: a prospective study.** *Stroke* 1987;18:997–1004
17. Earnest F, Forbes G, Sandok BA, et al. **Complications of cerebral angiography: prospective assessment of risk.** *AJR Am J Roentgenol* 1984;142:247–253

18. Essig M, Engenhart MV, Knopp M, et al. **Cerebral arteriovenous malformations: improved nidus demarcation by means of dynamic tagging MR-angiography.** *Magn Reson Imaging* 1996;14: 227–233
19. Aoki S, Nanbu A, Yoshikawa T, Hori M, Kumagai H, Araki T. **2D in thick-slice MR digital subtraction angiography with one-second temporal resolution: assessment of cerebrovascular disorders.** In: *Proceedings of the Annual Meeting of the American Society of Neuroradiology, 1999.* Oak Brook, IL: American Society of Neuroradiology; 1999:122
20. Wang Y, Johnston DL, Breen JF, et al. **Dynamic MR digital subtraction angiography using contrast enhancement, fast data acquisition, and complex subtraction.** *Magn Reson Med* 1996; 36:551–556
21. Maki JH, Prince MR, Chenevert TC. **Optimizing three dimensional gadolinium-enhanced magnetic resonance angiography: original investigation.** *Invest Radiol* 1998;33:528–537
22. Spetzler RF, Martin NA. **A proposed grading system for arteriovenous malformations.** *J Neurosurg* 1986;65:476–483
23. Redekop G, Terbrugge K, Montanera W, Willinsky RA. **Arterial aneurysms associated with cerebral arteriovenous malformations: classification, incidence, and risk of hemorrhage.** *J Neurosurg* 1998;89:539–546
24. Thompson RC, Steinberg GK, Levy RP, Marks MP. **The management of patients with arteriovenous malformations and associated intracranial aneurysms.** *Neurosurgery* 1998;43:202–212
25. Cloft HJ, Joseph GJ, Dion JE. **Risk of cerebral angiography in patients with subarachnoid hemorrhage, cerebral aneurysm, and arteriovenous malformation: a meta-analysis.** *Stroke* 1999; 30:317–320
26. Parker DL, Tsuruda JS, Goodrich KC, Alexander AL, Buswell HR. **Contrast-enhanced magnetic resonance angiography of cerebral arteries: a review.** *Invest Radiol* 1998;33:560–572
27. Ehricke HH, Schad LR, Gademann G, Wowra B, Endenhart R, Lorenz WJ. **Use of MR angiography for stereotactic planning.** *J Comput Assist Tomogr* 1992;16:35–40
28. Flamm CR. **Technology assessment of magnetic resonance angiography: why pretty pictures are not enough: an overview.** *Invest Radiol* 1998;33:547–552
29. Goodrich KC, Blatter DD, Parker DL, Du YP, Meyer KJ, Bernstein Ma. **A quantitative study of ramped radio frequency, magnetization transfer, and slab thickness in three-dimensional time-of-flight magnetic resonance angiography in a patient population.** *Invest Radiol* 1996;31:323–332
30. Du YP, Parker DL, Davis WL, et al. **Experimental and theoretical studies of vessel contrast-to-noise ratio in intracranial time-of-flight MR angiography.** *J Magn Reson Imaging* 1996;6: 99–108
31. Lunsford LD, Kondziolka D, Flickinger JC, et al. **Stereotactic radiosurgery for arteriovenous malformations of the brain.** *J Neurosurg* 1991;75:512–524
32. Oppenheim C, Meder JF, Trystram D, et al. **Radiosurgery of cerebral arteriovenous malformation: is an early angiogram needed?** *AJNR Am J Neuroradiol* 1999;20:475–481
33. Pollock BE, Flickinger JC, Lunsford LD, Maitz A, Kondziolka D. **Factors associated with successful arteriovenous malformation radiosurgery.** *Neurosurgery* 1998;42:1239–1247
34. Pollock BE, Lunsford LD, Kondziolka D, Maitz A, Flickinger JC. **Patient outcomes after stereotactic radiosurgery for "operable" arteriovenous malformations.** *Neurosurgery* 1994;35:1–8
35. Steiner L, Lindquist C, Adler JR, Torner JC, Alves W, Steiner M. **Clinical outcome of radiosurgery for cerebral arteriovenous malformations.** *J Neurosurg* 1992;77:1–8
36. Betti OO, Munari C, Rosler R. **Stereotactic radiosurgery with the linear accelerator: treatment of arteriovenous malformations.** *Neurosurgery* 1989;24:311–321
37. Columbo F, Benedetti A, Pozza F, Marchetti C, Chierego G. **Linear accelerator radiosurgery of cerebral arteriovenous malformations.** *Neurosurgery* 1989;24:833–840
38. Steinberg GK, Fabrikant JI, Marks MP, et al. **Stereotactic heavy-charged-particle Bragg-peak radiation for intracranial arteriovenous malformations.** *N Engl J Med* 1990;323:96–101
39. Friedman WA, Blatt DL, Bova FJ, Buatti JM, Mendenhall WM, Kubilis PS. **The risk of hemorrhage after radiosurgery for arteriovenous malformations.** *J Neurosurg* 1996;84:912–919
40. Colombo F, Pozza F, Chierego G, Casentini L, Giampaolo DL, Francescon P. **Linear accelerator radiosurgery of cerebral arteriovenous malformations.** *Neurosurgery* 1994;34:14–20
41. Hennig J, Scheffler K, Laubenberger J, Strecker R. **Time-resolved projection after bolus injection of contrast agent.** *Magn Reson Med* 1997;37:341–345
42. Pollock BE, Kondziolka D, Flickinger JC, et al. **Magnetic resonance imaging: an accurate method to evaluate arteriovenous malformations after stereotactic radiosurgery.** *J Neurosurg* 1996;85:1044–1049